STUDY ABOUT THE CORROSION OF STRUCTURAL MATERIALS IN PB-BI EUTECTIC AND COOLANT OXIDATION

ANDREI VILCU [1], KONDO MASATOSHI [2], MINORU TAKAHASHI [2], ADHI PRIBADI MUMPUNI [3]

[1] Institute for Nuclear Research (RATEN ICN) Pitesti, Romania
[2] Tokyo Institute of Technology, Tokyo, Japan
[3] Jakarta State Polytehnic
e-mail: andrei.vilcu@nuclear.ro

Abstract

The use of lead (Pb) based liquid metal alloys have been proposed as candidate coolants for GEN IV fast reactors (LFR) and accelerator driven systems (ADS). This study focuses on one of the main problems of this technology: structural materials compatibility with the coolant at high temperature. One of the proposed methods to mitigate the corrosiveness of lead based coolants is to control the oxygen concentration within specific limits in order to passivate the structural materials. To investigate this problem two corrosion tests have been performed using the Pb-Bi Circulation Loop at Tokyo Institute of Technology and a "melting pot" corrosion test (static conditions). The steel specimens used for these experiments were welded using the TIG method in the following configurations: SUS316L - SUS316L, HCM12A - HCM12A, SUS316L -HCM12A.This study will present the experience gained from these corrosion tests, with emphasis on the procedures, technology used and the main problems that have been faced during loop operation.

Keywords: *Corrosion, Weld joints, Lead-Bismuth, Oxygen sensor, Coolant oxidation*

Introduction

Lead-cooled fast reactors and Accelerated-driven systems are candidates for the Generation-IV nuclear systems. Lead and lead-bismuth eutectic (LBE) are promising coolants, due to high atomic mass, low absorption cross section, high boiling point and good heat transfer proprieties. However, Pb and LBE are corrosive to structural and cladding candidate steels. To mitigate the corrosive nature of the coolant, the passivation of steels with regenerating oxide scales has been proposed by which requires an active control of the oxygen dissolved in the coolant. But this method can only be applicable in moderate operating temperatures (< 480 °C), limiting the efficiency of the system.

For nuclear structural materials, welding technology is an indispensable process. Tungsten Inert Gas (TIG) welding is one kind of high quality technology used. When steels are welded, microstructural changes occur in the fusion zone and heat affected zones (HAZ), which might affect the corrosion resistance. In the case of heat affected zones, there is an increased complexity regarding microstructural changes: coarse-grained HAZ, fine-grained HAZ, inter-critical HAZ, and subcritical HAZ. It has been shown that welded materials have a susceptibility to liquid metal embrittlement and the corrosion rate of the weld is higher because of the depletion of Cr near the surface of the weld.

Corrosion consists of selective dissolution of alloying elements (Ni, Cr, Fe) in the grain boundary (inter-granular attack) and this process is simultaneous with LBE penetration. As LBE penetrates through the grain boundary, dissolution and penetration might also occur in the grain (trans-granular attack). Both of these processes deteriorate the mechanical properties of the material, causing embrittlement of the material. Weld joints might represent one of the weakest points in a structural material, because of the microstructural and mechanical variations caused by the welding process.

This research focuses on the corrosion of welded austenitic steel 316L and ferritic-martensitic steel HCM12A, specifically the following pair of weld joints: 316L – 316L, HCMA12A – HCM12A, SUS316L – HCM12A (Dissimilar joining).

Materials

Chemical compositions for the specimens and filler rods used can be seen in Tables 1 and 2. Table 3 contains the types of weld joints used in present study.

HCM12A is a candidate material for the fossil fuel power plants and 316L is a material that will be used for the reactor vessel in lead or LBE-cooled systems.

As filler rod material, the following materials were used:
- TIG316L, used for joining 316L austenitic steels
- TIG410, used for joying HCM12A ferritic steels
- TIG309, used for dissimilar joining of HCM12A and SUS316L.

Table 1. Chemical compositions of steels (wt%)

Steel	Cr	Ni	C	Mo	W	Si	Others
316L	16.0 – 18.0	10.0 – 14.0	0.08	2.0 -3.0	-	1.0	Mn - 2.0, N - 0.1, P - 0.045, S - 0.03
HCM12A	11.0	-	0.11	0.4	2.0	0.1	Mn - 0.6, N - 0.06, Cu - 1.0, V - 0.2, Nb - 0.05

Table 2. Chemical composition of TIG welding rods (wt%)

Rod	C	Si	Mn	Mo	Ni	Cr	P	S	Cu
TIG316L	0.03	0.3 – 0.65	1.0 – 2.5	2.0 – 3.0	11.0 – 14.0	18.0 – 20.0	0.03	0.03	0.75
TIG410	0.1	0.4	0.4	0.2	0.1	13	0.015	0.02	0.2
TIG309	0.03	0.3 – 0.65	1.0 – 2.5	0.75	12.0 – 14.0	23.0 – 25.0	0.03	0.03	0.75

Table 3. Types of weld joints used

Weld Joint	Experiment type	Weld Rod
316L – 316L	Static and Dynamic	TIG316L
HCM12A – HCM12A	Static and Dynamic	TIG410
HCM12A – 316L	Static and Dynamic	TIG309
316L – 316L	Only static	TIG410

Before the welding procedure, the specimens have been mechanically polished so they would have the same surface roughness of about 1.5 µm. After this procedure, the specimens have been welded by the TIG method, at a traveling speed of 150 mm/min and a current of 40A. For the flowing condition, the specimens have been mechanically polished again in order to remove the dent from the fusion zone, because it would of probably produced turbulent flow and might of accelerated the corrosion.

Experimental apparatus and procedures

Loop experiment

Fig. 1 shows the Pb-Bi forced convection experimental apparatus that is used for corrosion and erosion tests. In Table 4 the planned experimental conditions are presented.

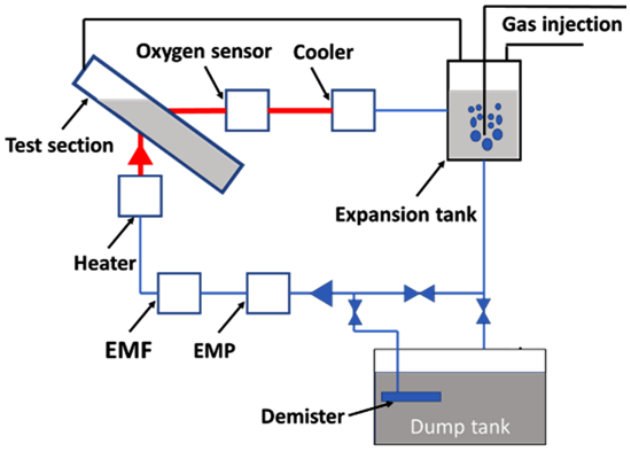


Fig. 1. Bird's eye view of the Pb-Bi forced convection loop

Table 4. Experimental conditions for Pb-Bi loop

Flow-rate	3 L/min
Velocity	1 m/s
Temperature in hot region (test section)	480 °C
Temperature in cold region	400 °C
Test time	1000 h
Oxygen concentration	10^{-7} wt%

Calibration of the EMF

Before starting the corrosion test, a calibration of the Electro-Magnetic Flowmeter (EMF) was necessary. The principle of the EMF is that an applied magnetic field will be modified by the flow, so the voltage difference is proportional to the flow-rate. The calibration is required because the corrosive environment might dissolve the electrodes. Also, the corrosion products from the structural materials of the loop might adhere on electrode surface.

In order to calibrate the EMF, the level of LBE in the loop has to be known. The expansion tank is equipped with 3 electrodes that are used for indicating the level: High, Medium and Low. Firstly, it is necessary to evacuate the loop and then start inserting high purity Argon gas (99.9999 %). This process is repeated around 4 times in order to make sure that the oxygen in the loop is at an adequate concentration. Then, the loop and the dump tank are heated till a temperature of 250 °C.

The LBE is charged into the loop by pressurizing the dump tank with Argon gas. When the level of LBE is at the High indication, the valve is closed leaving the LBE in a stationary condition.

The volume of the Expansion tank and the distance between the High electrode and Medium electrode is known, so the flow-rate can be measured by measuring the time that the level goes from High to Medium. But, in order to get accurate data, the flow-rate has to be constant; this can be done by connecting the gas line of the expansion tank with that of the dump tank.

After this, the LBE was dumped back into the dump tank, by opening a valve. The output voltage of the EMF is connected to a data acquisition system, so the voltage for a specific flow-rate can be obtained.

Data for six values of the flow-rate were gathered and the results show a linear function (as shown in Figure 2). This function was then inputted in the instrumentation and data acquisition system.

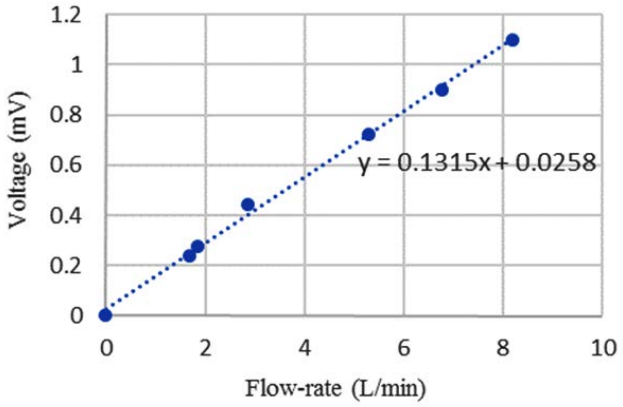


Fig. 2. Flow rate calibration

Corrosion test procedures

Before starting the corrosion test, the specimens were cleaned with acetone and ethanol in an ultrasonic bath. After this, the specimens were inserted in a Molybdenum holder and then placed in the loop (as in Figure 3).

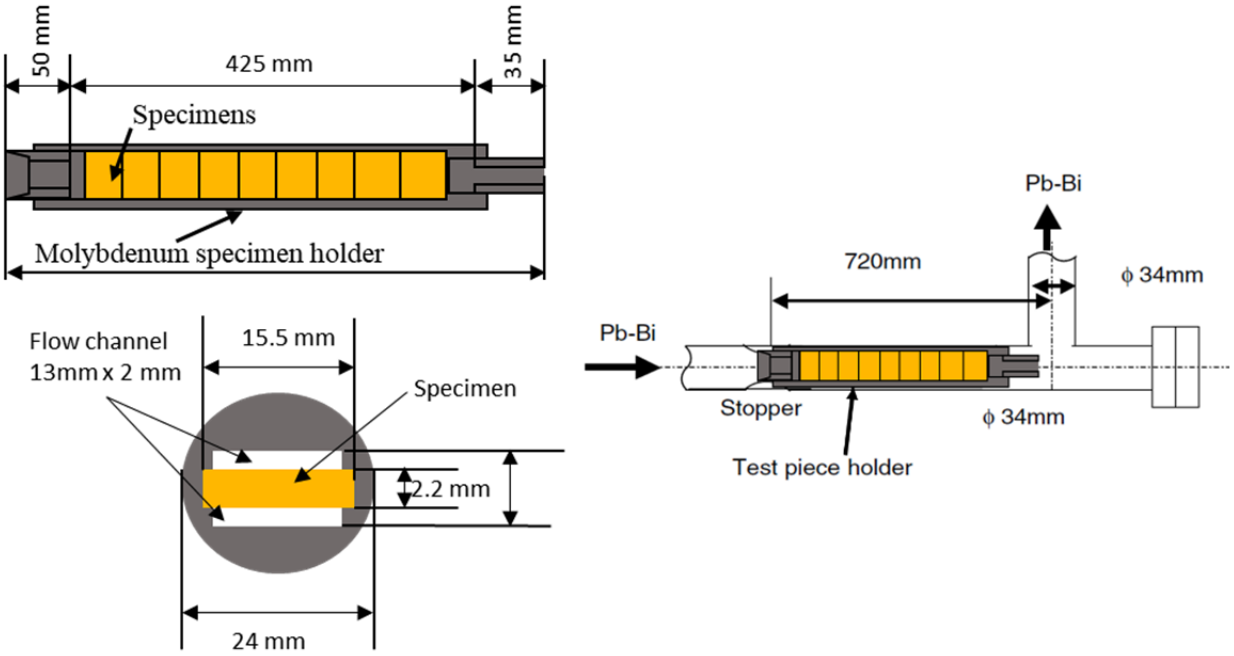


Fig. 3. Schematic view of test section and piece holder ration

The LBE in the dump tank was melted at 180 °C for several days in order for the impurities to float at the surface of the LBE due to buoyancy force. The loop is evacuated and then filled with high purity Argon several times. Then the LBE is charged into the loop at 180 °C. The oxygen solubility for this temperature is approximated by using the following relation:

$$\log (S, \text{wt.}\%) = 2.25 - 4125/T \text{ in LBE} \qquad (1)$$

with T in (K) and 673 K < T < 1 013 K.

By extrapolation, the value for 180°C can be approximated to be about 10^{-7} wt%. The dissolved oxygen concentration is satisfactory because it is above the magnetite formation potential and below the Lead oxide (PbO) potential formation. Thus, the protective and regenerative oxide layer can be ensured and the coolant will not oxidize. The limits for the oxygen concentration can be seen in Figure 4 taken from [1].

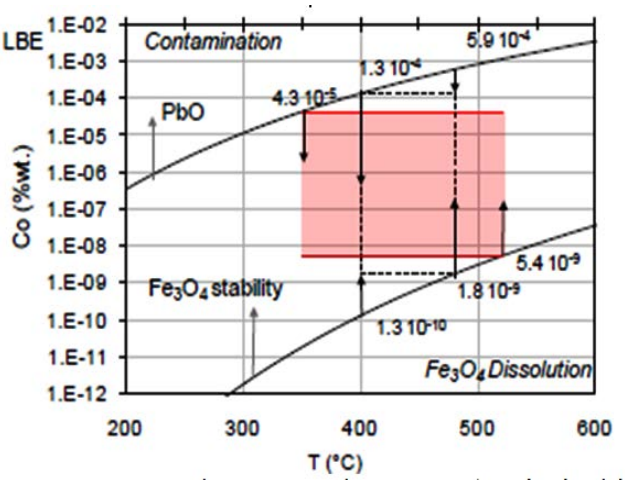


Fig. 4. Oxygen concentration appropriate range (marked with red), [1]

Charging the LBE in the loop was started by pressurizing the dump tank with Argon gas. The pressure needs to be increased slowly, so the impurities at the surface of the LBE won't mix in the melt. The LBE is charged slowly in the loop, at a flow-rate of approximately 0.6 L/min. When the appropriate level was achieved, the loop is heated up till 250 °C through electrical heaters placed on the surface of the loop pipes. Then, start circulating the LBE through the use of the electro-magnetic pump. When the value of 1 m/s was achieved, the temperature was increased to 400 °C. Then, it start operating the high power heater and the cooler, setting the test section region at 480 °C and 400°C for the rest of the loop. Generally, impurities in the system tend to accumulate at the cold spots because of the difference in solubility between the hot spot (higher solubility) and the cold spot (lower solubility). It was observed (see Figure 5) that accumulation of impurities affected the thermal-hydraulic performances of the loop.

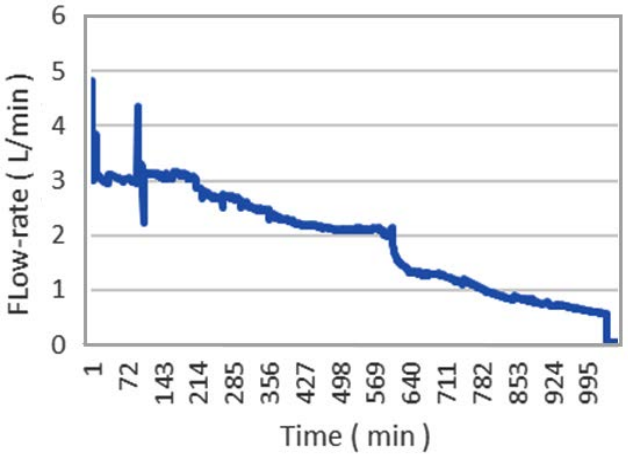


Fig. 5. Effect of impurity accumulation on flow-rate

It can be seen from the figure that impurity accumulation in cold regions caused very large pressure drops. Because of this, the pump voltage needed to be increased in order to achieve the desired velocity of 1 m/s.

Oxygen measurement

The dissolved oxygen concentration was measured with two solid electrolyte oxygen sensors. The solid electrolyte material is made of Yttria Stabilized Zirconia (YSZ) and the reference electrode is made from a solid powder that is made from a mixture of iron and magnetite (Fe / Fe_3O_4). The oxygen sensor was mounted downstream from the test section in order to measure the oxygen potential in the loop. More details about the oxygen sensor can be seen in the static experiment section.

Coolant oxidation accident

Initially, it was suspected that the large pressure drops were because the precipitations plugged the narrow channel of the test section. The operation was stopped and the test section was removed to observe if this is the case. No precipitations were observed in the test sections, the experiment was restarted. After restarting the experiment, the condition of the loop became worse. Thermal-hydraulic performance was poor and thermocouple signals were very strange. As an example, the thermocouple that controlled the cooler temperature showed a temperature of 200 °C, but the cooler did not do any work to achieve this temperature, basically the cooler was not functioning. The condition became obvious and the signal from the oxygen sensor confirmed that the oxygen concentration inside the loop was near the saturation point at 480 °C (10^{-3} wt% indicating that the coolant might of oxidized).

It can be seen from Figure 6 that the heat exchange capabilities greatly decreased because of the accumulation of coolant oxides.

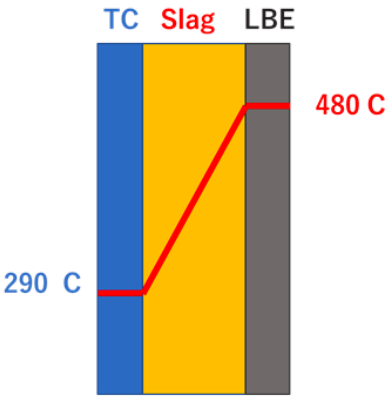


Fig. 6. Large fouling effect on the thermocouple (TC)

An apparent fouling effect was also present on other thermocouples in various locations: inlet of test section, outlet of test section, oxygen sensor (see Figure 7) and cooler. Because of this, the experiment has been stopped to accurately investigate what happened. By opening the oxygen sensor compartment, a lot of coolant precipitations were observed (see Fig. 7): PbO and probably Bi oxides.



Fig. 7. Coolant oxide precipitation in the loop and on a thermocouple well

This situation occurred because of a blockage inside the gas line. Because there was a blockage, it could not evacuate the gas or supply pure Argon gas. At first, the experimentalists were not aware of this, they thinking that the indication of the pressure gauge was correct. Thus, the gas space inside the loop was in fact air, causing the coolant to oxidize.

Why there is a blockage inside the gas line is open to speculation, until the situation is properly investigated. From previous experience it was known that LBE may form black dust through the evaporation, condensation and accumulation of aerosols. The authors' assumption is that black dust accumulated with time inside the vapour trap, causing the blockage.

It is known that coolant oxidation and precipitation may be solved by bubbling Hydrogen with an inert gas (Argon or Helium). Through the combined reduction and mechanical impact of the bubbles, the coolant can become clean, fully restoring operating conditions. Unfortunately, the Argon and Hydrogen gas bubbling line was plugged. Because of this, the experiment had to be stopped and further repair awaits the Pb-Bi forced convection loop.

Static experiment

To investigate the effects of corrosion in a static condition, a simple apparatus was constructed. Details regarding the experimental apparatus and conditions can be seen in the figure and table presented below.

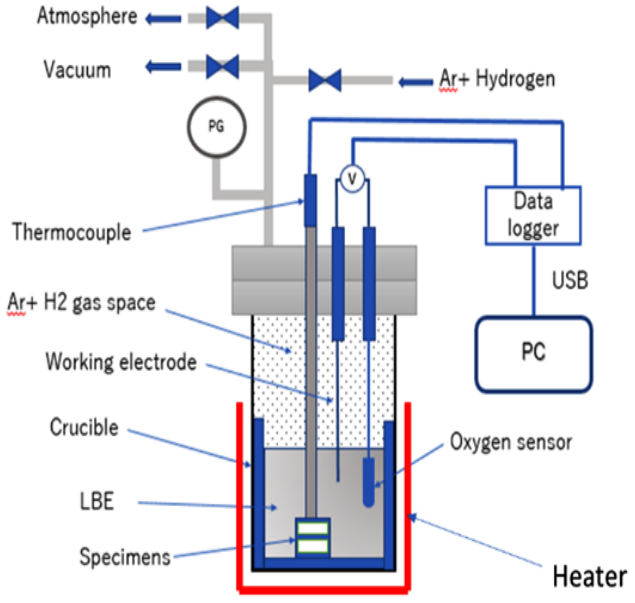


Fig. 8. Schematic view of static experiment

Table 5. Experimental conditions for static test

Temperature	480 °C
Oxygen concentration	10^{-8} wt%
Time	500 h

Firstly, LBE was melted to the temperature of 150 °C. During this process a lot of impurities accumulate at the surface, so it is necessary to remove the impurities mechanically. When the condition was good, the specimens were inserted in the LBE. Because of the buoyancy force of LBE the specimen holder was attached to the thermocouple by a wire.

Oxygen measurement

The oxygen measurement was made with a Magnesia stabilized Zirconia (MSZ) solid electrolyte and the reference electrode is made of a solid powder mixture of Fe and Fe_3O_4. Figure 9 shows the structure of the oxygen sensor that was fabricated for this experiment.

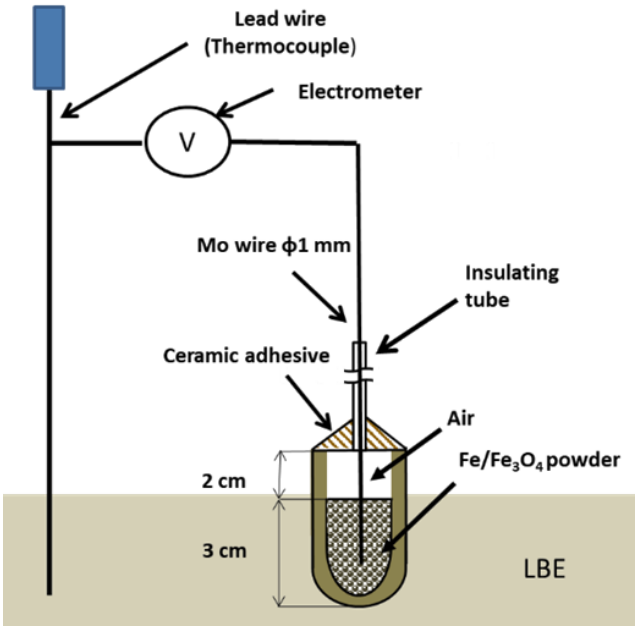


Fig. 9. Schematic drawing of oxygen sensor

Table 6. Oxygen sensor specifications

Solid electrolyte	MSZ
Reference electrode (solid powder)	Fe / Fe_3O_4
Mass ratio of powder	3(Fe) : 1(Fe_3O_4)
Total mass	2.84 g

Because there is an oxygen partial pressure difference across the solid electrolyte there will be an oxygen ion conduction inside the electrolyte. This conduction establishes an EMF that can be measured. To obtain the oxygen concentration, the Nernst equation for the cell potential at equilibrium is used:

$$E = \frac{RT}{4F} \ln \frac{P''_{O_2}}{P'_{O_2}} \qquad (2)$$

where E is the measured EMF (V), R is the universal gas constant, F is the Faraday constant, T is the absolute temperature of the sensor (K), P''_{O_2} is the partial pressure of oxygen in the reference side and P'_{O_2} is the partial pressure on the working electrode side (LBE).

The oxygen partial pressure in the reference side (Fe/ Fe_3O_4) can be calculated by:

$$\frac{RT}{2}\ln P''_{O_2} = \frac{\Delta G^0_{Fe_3O_4}}{4} \quad (3)$$

where $\Delta G^0_{Fe_3O_4}$ is the Gibbs free energy for formation of Fe_3O_4, , expressed in J/mol.

From the expression of the oxygen activity, the oxygen partial pressure in LBE can be obtained:

$$\left(P'_{O_2}\right)^{1/2} = C_O \exp\left(\frac{\Delta G^{EX}_{0,LBE}}{RT}\right) \quad (4)$$

where $\Delta G^{EX}_{0,LBE}$ is the excess molar Gibbs free energy of dissolution of oxygen.

By substituting Eqs. (1), (2) and (3), we can obtain the cell potential for (Fe/ Fe_3O_4) mixture at equilibrium:

$$E = \frac{RT}{2F}\left(\frac{\Delta G^0_{Fe_3O_4}}{4RT} - \frac{\Delta G^{EX}_{0,LBE}}{RT} - \ln C_O\right) \quad (5)$$

Because a thermocouple was used as a lead-wire, it needs to consider the thermoelectric effect caused by the high temperature. The following correction has to be applied:

$$E_{cor} = E - \frac{-6.91 + 0.01762T}{1000} \quad (6)$$

Specimen analysis

At this moment, the only experiment from where it can be obtain data is the static one, but it is still under operation. First of all, after the experiment will be completed, the specimens will be covered with LBE, so in order to remove the residual LBE, without removing the oxide layers, it is necessary to immerse the specimens in a glycerine pool at 180 °C. After this, the glycerine will be cleaned with hot water at 80 °C.

In order to determine the corrosion rate, the first step is to measure the weight-loss. Before the corrosion test, the specimens were measured using an electronic balance with an accuracy of 0.1 mg. After this, the specimens will be cut, mounted into a special resin and mechanically polished. The cross section of the samples will be observed using the light-optical microscope, scanning electron microscope and energy dispersed X-ray analysis.

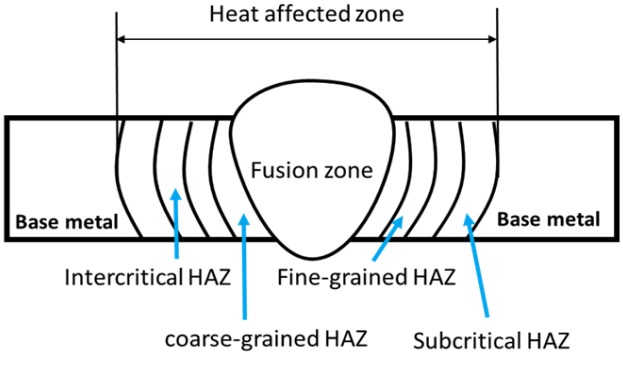


Fig. 10. Microstructural changes due to welding

The observations will be focused on the corrosion effect in the different areas of the heat affected zone, where microstructural changes might affect the corrosion rate and oxide layer depth. Geometrical details regarding the microstructural changes can be seen in Figure 10.

Oxygen pumping method

An alternative oxygen concentration control method in LBE is to use the electrochemical oxygen pumping (EOP).

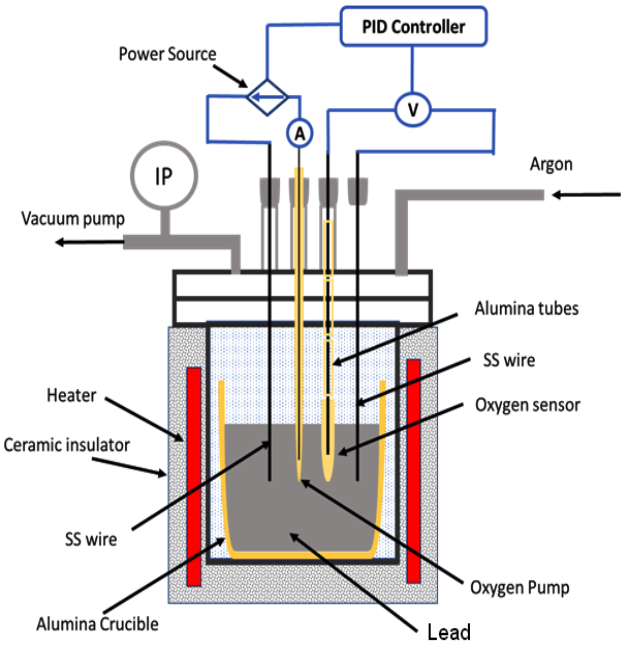


Fig. 11. Apparatus for oxygen pump testing

For the EMF measurement, a high impedance electrometer is required (> 10^{10} Ohm). These devices are expensive, so a custom device was designed using easy to find and cost effective parts (see Figure 12).

The oxygen concentration is controlled through a PID algorithm by a programmable voltage source. The pumping of oxygen in and out of the lead alloy will be done by reversing the voltage polarity. The voltage should not exceed the reducing potential of Zirconia (2.5 V).

The applied electric potential (V) should be higher than the Nernst potential (Vn) which is generated by the difference of chemical potential of oxygen. The oxygen flux will be proportional to this over-potential:

$$I = \frac{V - Vn}{Rs} \quad (7)$$

This technology has its limitations. If the voltage induced is too high, there will be a partial electrolysis of the electrolyte, so the voltage should not exceed the thermodynamic decomposition voltage of zirconia (2.5V at 500 ºC.

New research paths for the qualifications of a better material should be pursued.

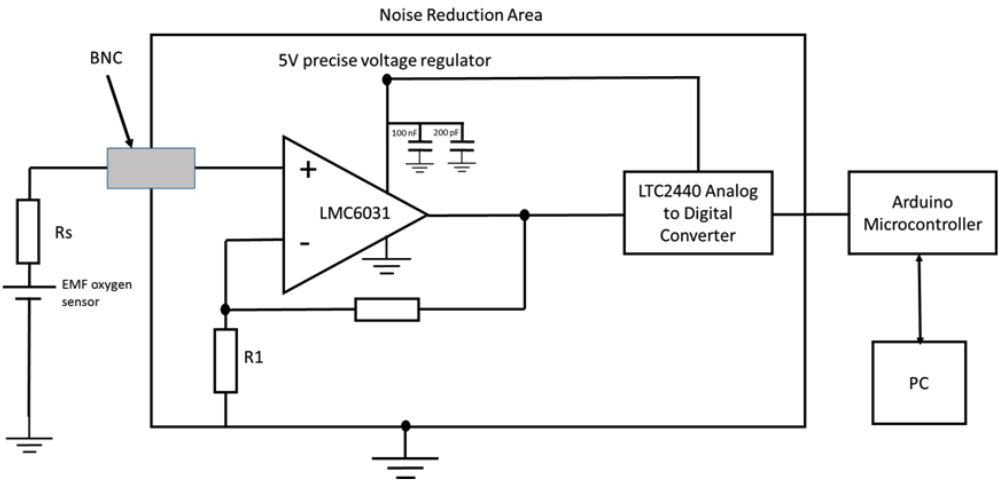


Fig. 12. Oxygen Sensor Electrometer

Conclusions

The study sustain that one of the most severe accidents in a lead alloy coolant based system, would be air ingress that eventually causes the coolant to oxidize.

It was observed that coolant oxides have a tendency of precipitating in cold spots and this greatly affects thermal-hydraulic performances causing large pressure drops and reducing the heat exchange capabilities.

Because the thermocouple measurements were flawed, it made the following systems to function poorly: pre-heaters, main heater, cooler, electro-magnetic pump and oxygen sensor measurement.

Every lead alloy cooled reactor design should take into consideration this accident, because it might cause coolant plugging, blockage of control rods, blockage of safety rods and oxide accumulation on the steam generator that will greatly affect the heat exchange capabilities.

Great care should be taken regarding the gas system of the reactor and periodic checks should be made, in order to ensure that coolant vapour does not accumulate.

References

[1] NEA-OECD, (2015) "Handbook on Lead-bismuth Eutectic Alloy and Lead Properties, Materials Compatibility, Thermal-hydraulics and Technologies", NEA 7268, Paris, France

[2] Wang, J., Rong, L., Li, D., Lu, S. (2016) "Effect of welding thermal cycles on the oxidation resistance of 9 wt% Cr heat resistant steels in 550 °C lead-bismuth eutectic", *Applied Surface Science*, No. 389, pp. 930-941

[3] Gromov, B., Orlov, Y.I., Martynov, P., Ivanov, K., Gulevsky, V. (1995) "Physical - chemicall principles of lead-bismuth coolant technology", in *Liquid Metal Systems*, Springer, pp. 339–343

[4] Andrén, H.O., Cai, G., Svensson, L.E. (1995) "Microstructure of heat resistant Chromium steel weld metals", *Applied Surface Science*, No.87–88, pp. 200–206

[5] Van den Bosch, J., Coen, G., Van Renterghem, W., Almazouzi, A. (2010) "Compatibility of ferritic–martensitic steel T91 welds with liquid lead–bismuth eutectic: Comparison between TIG and EB welds", *Journal of Nuclear Materials*, Vol. 396, pp. 57–64

[6] Kondo, M., Takahashi, M., Suzuki, T., Ishikawa, K., Hata, K., Qiu, S., Sekimoto, H. (2005) "Metallurgical Study on Erosion and Corrosion Behaviors of Steels Exposed to Liquid Lead-Bismuth Flow", *Journal of Nuclear Materials*, Vol. 343, pp. 349-359

[8] Kondo, M., Takahashi, M., Sawada, N., Hata, K. (2006) "Corrosion of Steels in Lead–Bismuth Flow", *Journal of Nuclear Science Technology*, Vol. 43, No.2, pp.107-116